Modeling Shielded Pickup Measurements for Aluminum Test Chambers with ECLOUD

Emily A. Hemingway
St. Olaf College, Northfield, MN, 55057
(Dated: August 11, 2012)

One of the goals of the Cornell Electron Storage Ring Test Accelerator (CesrTA) program is to study electron cloud development in the CESR ring and explore mitigation techniques aimed at reducing the effects of electron clouds and improve the performance of the accelerator. By using time-resolved shielded pickup measurements in conjunction with a customized electron cloud modeling program called ECLOUD, the effects of beam conditioning on different kinds of beampipes can be investigated. This analysis technique has already been used to study conditioning effects in chambers coated with amorphous carbon. An updated optimized simulation for shielded pickup signals in bare aluminum test chamber as been developed so that a similar analysis can be carried out with aluminum. SPU measurements for unconditioned aluminum will be carried out mid-August of this year and conditioned measurements will be conducted in November. The measurements used in this report were taken in a conditioned vacuum chamber in May of 2010.

I. INTRODUCTION

The formation of an electron cloud, the accumulation of electrons inside the beampipe of a particle accelerator, begins with the production of primary electrons. Some primary electrons may be produced by the ionization of residual gas inside the beampipe, but for positron and electron beams, most are photoelectrons produced via the photoelectric affect when synchrotron radiation strikes the walls of the beampipe[1]. Secondary electrons are produced when electrons collide with the wall. The total secondary yield (SEY), the number of electrons produced per incident electron) has three components: rediffused yield (δ_R), elastic yield (δ_E), and true secondary yield (δ_{TS}). The type of secondary electron produced is dependent upon the kinetic energy and angle of the incident electron. An example of a typical SEY energy dependence curve is shown in Fig. 1[2]. As this curve shows, the elastic reflection process dominates at low incident energy while the true secondary process dominates at high incident energy. The secondary electrons produced the true secondary process have low kinetic energy. The elastic reflection process conserves kinetic energy. Rediffused secondary electrons are produced with intermediate kinetic energy [2].

The density of the electron cloud in a beampipe can increase rapidly through a phenomenon called multipacting. Multipacting occurs when electrons from the cloud are accelerated by the electric field of a passing beam bunch to a high enough energy such that more than one secondary electron is produced when it strikes the wall [2]. Dense electron clouds can interfere with the operation of the accelerator and beam quality and cause beam loss. Therefore, study of electron cloud behavior and the development of mitigation techniques is important for the future of accelerator-based science and research.

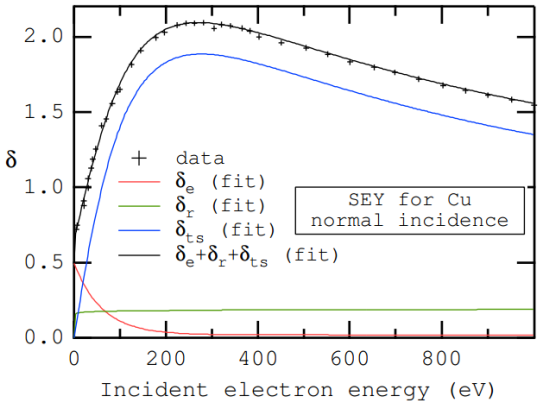

FIG. 1: *Secondary yield components for Cu*: An example of a typical SEY curve from Ref. [2].

II. SHIELDED PICKUP DETECTORS

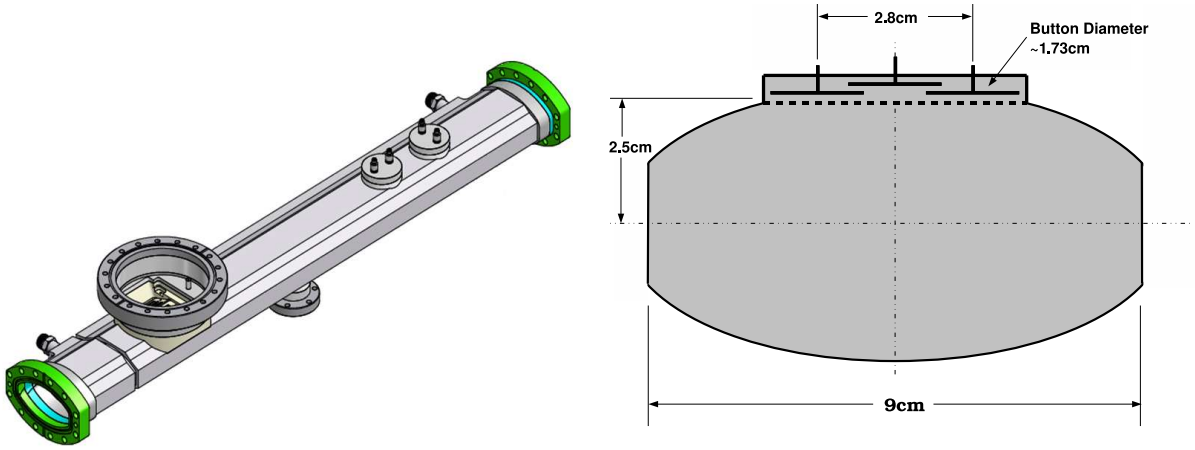

FIG. 2: *Shielded pickup detectors*: The figure on the left shows a beampipe equipped with two pairs of shielded pickup buttons. The figure on the right gives a cross-sectional view of the beampipe with the SPU buttons.

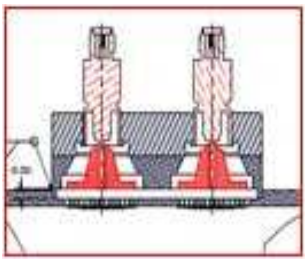

FIG. 3: *Cross section of a pair of SPU electrodes*

The detectors used to collect the data presented in this report are called shielded pickup (SPU) detectors. SPU's are very similar beam to position monitors with one major difference: the electrodes in SPU's are removed from the beampipe by an array of holes in the top

of the chamber (seen in the cross-sectional views in Fig. 2 and 3). The holes are 0.76 mm in diameter and have a depth-to-diameter ratio of 3:1. This serves to shield the electrodes from the direct signal induced by the passing beam [3]. Electrodes are biased at +50 V so that any low-energy secondary electron created on the surface of the electrodes do not escape into the beampipe. Signals induced by electrons from the beampipe drifting through the holes and hitting the electrodes pass through a voltage gain of 100 before being recorded by an 8-bit digitizing oscilloscope with 50 Ω input impedance in 0.1 ns time steps [3]. Pairs of electrodes are mounted perpendicular to each other on top of the beampipe (see Fig. 2) such that electrodes are located at 0 and ±14 mm from the horizontal center of the chamber. For the studies conducted in this report, data from one of the central electrodes was used.

III. ECLOUD

ECLOUD is a program designed to simulate the build up of electron clouds that was first developed at CERN in the 1990's. It has been actively developed at Cornell since 2008. In 2010, ECLOUD was adapted to simulate SPU measurements [4].

Input parameters include characteristics of the beam, geometry of the beampipe, and properties of the beampipe material (such as quantum efficiency and secondary emission yield) [6]. Parameters for photoelectron generation, SEY, and beam dynamics (magnetic fields, beam kicks, and space charge forces from cloud electrons) [3].

Using discrete timesteps, ECLOUD is able to model the development of the electron cloud with time. Rather than doing this with individual electrons, ECLOUD utilizes macroparticles. These macroparticles have the same energy to mass ratio as electrons but carry the charge of thousands of electrons. When these macroparticles collide with the wall of the beampipe, their charge changes in accordance with the input SEY model. When macroparticles hit an SPU detector, a portion of the charge contributes to the simulated signal while the rest undergoes SEY processes. The number of marcroparticles that contribute to a signal during a particular time slice determines the size of the statistical error of the signal. The smaller the number of marcroparticles, the greater the uncertainty.

IV. MOTIVATION

A study of the conditioning of test chambers coated with amorphous-carbon was conducted using SPU measurements in conjunction with ECLOUD simulations (shown in Fig. 4)[3, 4]. SPU measurements for an unconditioned a-C-coated chamber with two positron bunches (with an energy of 5.3 GeV and bunch current of 3 mA) spaced 14 ns apart were taken in September of 2011 (shown as a blue dotted line in Fig. 4) and November 2011 (shown as a red dotted line). The signal recorded in November, after an increase in the chamber's exposure to synchrotron radiation from 4e20 γ/m to 6e24 γ/m, is clearly smaller than the unconditioned signal acquired in September.

An optimized model for September's unconditioned signal (shown in Fig. 4 as blue circles with error bars) was created in ECLOUD. By changing parameters in this optimized signal and comparing the resulting simulation to the signal measured in November, one can determine the effects of conditioning on the a-C-coated chamber.

In the model shown as green points, the SEY of the optimized was reduced by 50%. The second pulse of the simulated signal matches the size of the conditioned signal's second

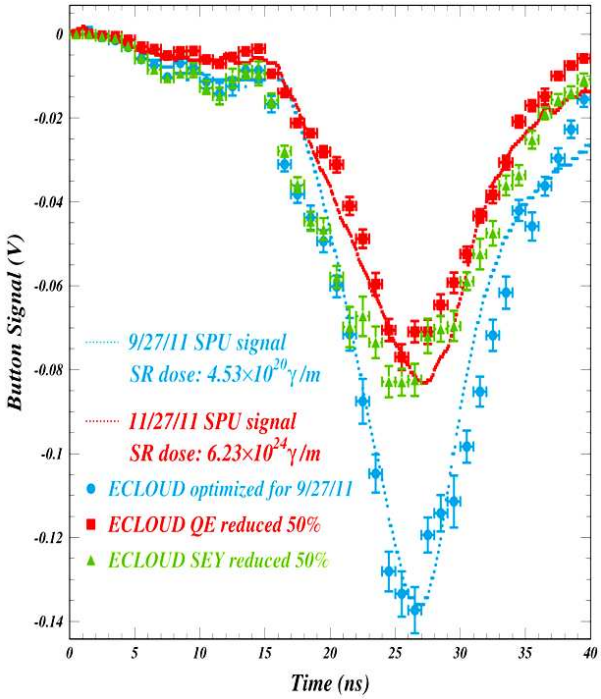

FIG. 4: *Conditioning of a chamber coated with amorphous-carbon*[3, 4]: The blue dotted line is the SPU signal measured in an unconditioned chamber in September 2011. The red dotted line is the SPU signal measured in November 2011. The optimized model for the unconditioned signal is shown in blue with error bars. The green simulation is the optimized model with a reduced SEY. The red simulation (with error bars) is the optimized model with a reduced QE.

pulse, however, the first remains the same size as the unconditioned signal's first pulse. If the QE is reduced by 50%, as shown in the red simulation (red circles with error bars), the simulated signal has good agreement with the measured conditioned signal. From this, it can be inferred that in a-C-coated chambers, the QE is affected.

This sort of analysis is very useful in determining the effects of conditioning in different kinds of test chambers. The goal of this research project is to update the optimized model for bare aluminum test chambers so that conditioning effects can be studied using this method. Unconditioned Al chambers with SPU detectors have been installed recently in the Cornell Electron Storage Ring. The SPU measurements for this unconditioned Al chamber will be taken mid-August 2012. Measurements will be taken again November 2012 after the chamber has been conditioned. Until the new measurements can be taken, simulations will be compared to existing Al chamber measurements recorded in May 2010 with two 5.3 GeV positron bunches with a bunch current of 3 mA.

V. RESULTS

The blue points in Fig. 5 shows the original optimized model for SPU measurements in an Al beampipe. This model gives reasonable agreement with the measured data. However, this model utilizes an older version of the ECLOUD program that makes assumptions that are not necessarily true to reality. The version of ECLOUD currently in use uses new photon

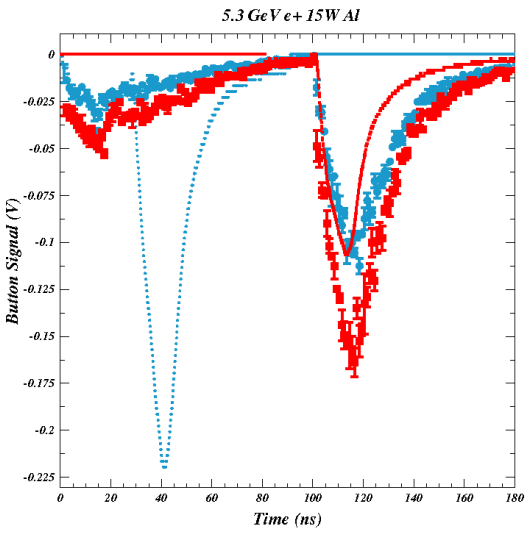

FIG. 5: *2011 model for Al*: The blue points shows an optimized model developed in 2011. The red points are the same parameters run with more realistic photon modeling and chamber profile. Both models were run with a bunch spacing of 100 ns.

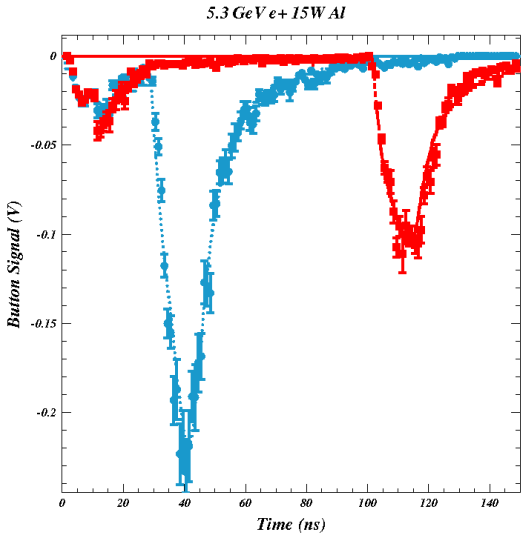

FIG. 6: *New model for Al*: The blue data and model have a bunch spacing of 28 ns. The red data and model have a 100 ns bunch spacing. The agreement between the models and measurements in both cases are far better than that shown in Fig. 5.

modeling results from Synrad3D (which models photon scattering throughout the whole ring and uses the results to determine the distribution of photoelectron production around the beampipe) and a more realistic chamber profile (an ellipse with cut-off vertical sides). The red model in Fig. 5 shows the same input parameters as the blue model run with this current version of ECLOUD. This model has some obvious problems: overall, the modeled signal is too big and it increases much too early. Furthermore, this model did not utilize updated SPU response functions and primary electron models.

Fig. 6 shows the new optimized model for SPU measurements in an Al beampipe. At first glance, this model is a clear improvement over the old model. Both the 28 ns bunch spacing and the 100 ns bunch spacing simulations give a good description of the measured signals. To achieve this, a new photoelectron energy distribution for electrons produced by reflected photons was used, secondary yield parameters and the quantum efficiency for reflected photons were adjusted and the horizontal beam position was shifted. These improvements are described in more detail below.

A. Photoelectron Energy for Reflected Photons

The shape of the first pulse is largely dependent upon the energy of photoelectrons produced on the floor by reflected photons. These photoelectrons have the most direct route to the SPU detectors and therefore arrive before photoelectrons from other parts of the beampipe. The most significant feature of the first pulse of the Al signal is the presence of two peaks within the first pulse. This resembles the first pulse observed in the SPU measurements for a-C-coated chambers. Following the example presented by the a-C

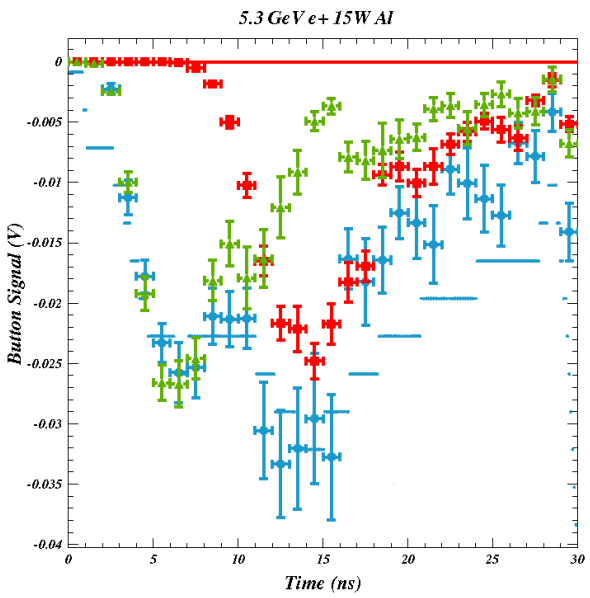

FIG. 7: *Components of the photoelectron energy for reflected photons*: The low-energy function is shown in red, the high-energy function is in green, and the combined effect of the two is shown in blue. The SPU measurements being simulated appear as blue horizontal lines (due to the least significant bit limitations of the oscilloscope).

simulation, the photoelectron energy for reflected photons is the sum of two power laws. Each power law is of the following form [4]:

$$f(E) = \frac{E^{P_1}}{\left(1 + \frac{E}{E_0}\right)^{P_2}} \tag{1}$$

$$E_0 = E_{peak}\left(\frac{P_2 - P_1}{P_1}\right) \tag{2}$$

The first power law, shown in red in Fig. 7, is a low-energy function with E_{peak}=8 eV, P_1=2.0, and P_2=9.0. The second power law, shown in green in Fig. 7, is a high-energy function with E_{peak}=100 eV, P_1=3.0, and P_2=6.3. The final, full first pulse, shown in blue in Fig. 7, is the sum of 25% of the first, low-energy power law and 75% of the second, high-energy function. The size of the first pulse can be adjusted by raising or lowering the quantum efficiency for reflected photons (the number of photoelectrons produced per absorbed photon).

B. Secondary Yield Parameters

The secondary emission yield makes a significant contribution to later portions of the SPU signal, particularly the second pulse. However, the component of the secondary yield that has the most influence upon the second pulse depends upon the timing of the second bunch. Soon after the first bunch passes, there are lots of high-energy electrons that can create true secondaries. As the cloud decays, more and more of the electrons have lower energies and elastic reflection becomes the dominant secondary emission process. This is

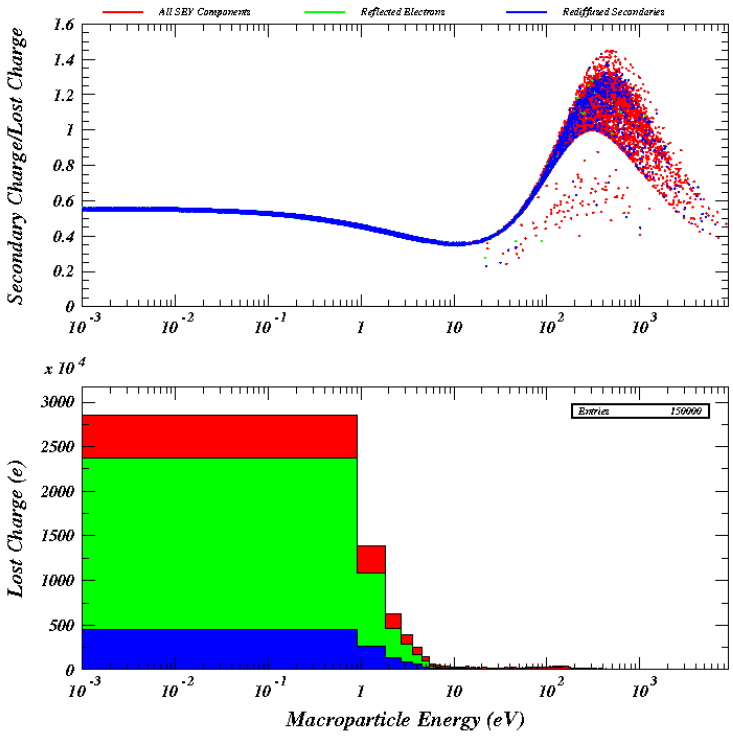

FIG. 8: *Secondary yield curve for the updated optimized model*: The upper plot shows the population of the SEY curve in as Fig. 1 for the case of the optimized Al model. The spread of the data in the y-direction shows the angular dependence of the secondary yield. All SEY components (mostly true secondaries at high energies) are plotted first in red. The elastic component is plotted second in green. The rediffused component is plotted last in blue.

why δ_{TS} tends to have more influence when the bunch spacing is small while δ_E has a greater effect at large bunch spacings.

In the case of aluminum, secondary yield parameters determined in surface physics measurements and in CesrTA tune shift measurements are as follows: $\delta_R = 0.2, \delta_E = 0.5, \delta_{TS} = 1.8$ [5]. The value of δ_R is quite close to the expected value at 0.2. δ_E is 0.5 as expected. δ_{TS}, on the other hand, is half of the expected value, 0.9. δ_{TS}-values greater than this gives a model for the second pulse that is too big.

C. Direct and Reflected Quantum Efficiencies

One of the main challenges in updating the optimized model for Al was reducing the size of the second pulse. One way this was attempted was by reducing the quantum efficiency for photons that strike the direct source point (shown in red in the cross-section in Fig. 9).

Because most of the first pulse comes from the floor of the beampipe, its size is determined by the quantum efficiency of photons that hit the floor. Photoelectrons created on the sides of the chamber have very little affect as they have a longer path and therefore do not contribute until the later part of the first pulse. Thus, the second pulse is more sensitive to the quantum efficiency of photons hitting the sides. Decreasing this value to a value much smaller than the QE for reflected photons resulted in models similar to that shown

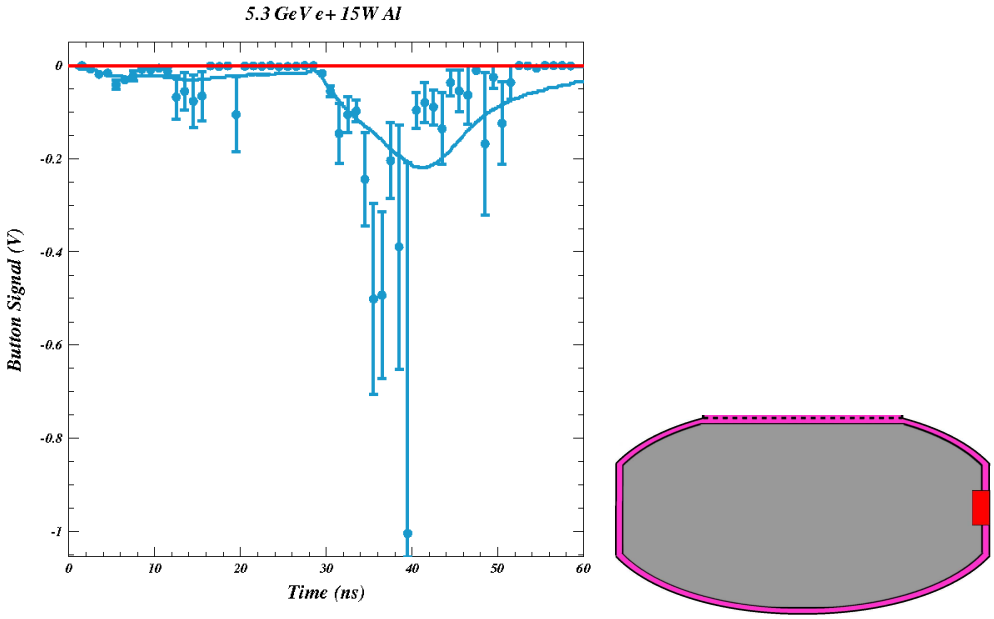

FIG. 9: *Two quantum efficiency components, small QER*: The quantum efficiency for photons that hit the wall at the direct source point (shown in red) is much smaller than the quantum efficiency for reflected photons. The result can be seen in the model on the left.

on the left in Fig. 9. The size of the second pulse was not reduced and the statistical error was dramatically increased. A possible explanation for this effect is that because decreasing the QE decreases the total charge of the cloud, there is less cloud-self repulsion into the detector. Fewer signal macroparticles contribute to the signal, so the statistical errors are larger. Because these fewer signal macroparticles have collided with the wall fewer times on their way to the detector, they carry more charge, thus giving the same-sized signal as many macroparticles with smaller charges [7].

A new feature of ECLOUD now allows for more flexible assignment of QE values. Separate quantum efficiencies can now be assigned for the direct source point, the point directly across from the direct source point, and the rest of the chamber (shown in Fig. 10). Because input QE values are averages over a range of absorbed photon energies and this spectrum varies with the number of photon reflections, it is reasonable that the QE's differ for the different types of photons absorbed on the bottom of the chamber versus the two sides. The three components can be plotted individually to show how the photoelectron production at different parts of the beampipe contribute to the total signal. Looking at the size of the component signals compared to the total signal (shown in blue in Fig. 10), it is interesting to see that the reflected component alone (shown in pink) is larger than the total signal. It would seem that photoelectrons from the sides of the beampipe serve to "block" the signal from the floor, reducing it to the correct size when the right balance of quantum efficiencies is achieved.

D. Beam Position

One parameter that had a substantial effect on the ECLOUD simulation of aluminum was the beam position. In Fig. 11, the red model shows the simulation with the beam in its

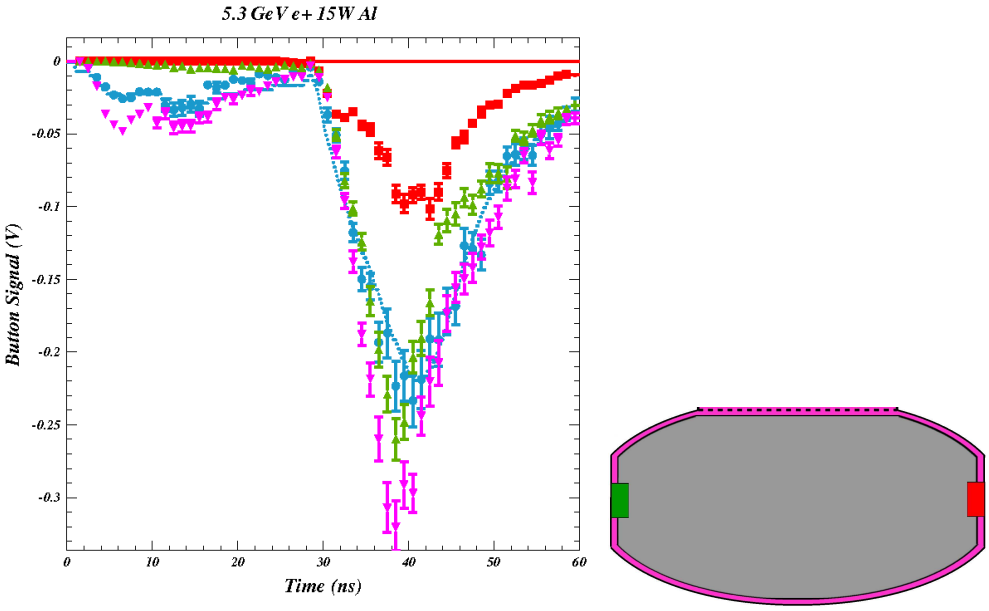

FIG. 10: *Two quantum efficiency components, small QER*: Quantum efficiency at the direct source point (red) is 0.16. QE at the point across from the direct point (green) is 0.2. QE everywhere else (pink) is 0.24. The signal created by each of these components is shown in the plot. The "sum" of these three components is shown in blue.

"original" position of 2.2 mm offset from the center (closer to the primary source point). In the blue model in Fig. 11, the beam is shifted 4 mm to a position of -1.8 mm (away from the primary source point). The effects of this change on the second pulse are quite dramatic. Attempts to produce a similar effect by altering other parameters were unsuccessful.

The second pulse of the signal is sensitive to the cloud spacial distortion when the second bunch arrives. The second bunch accelerates cloud particles directly below the beam axis when it passes by the detector. Further study of the cloud distribution in the locale of the beam are needed to understand this further.

VI. CONCLUSION

The model shown in Fig. 6 has good agreement with current SPU measurements of electron clouds in bare aluminum test chambers. Work remains to understand why the SEY model used in this optimized model differs from other reported SEY values for Al chambers.

A. Future Work

SPU data for unconditioned Al will be collected Mid-August. Upon fitting the model presented in this report to this new, unconditioned signal, it may be that δ_{TS} can be raised to a value closer to what is expected for bare Al.

In November, SPU measurements of the same chamber, now conditioned by exposure to synchrotron radiation, will be taken again. The new optimized model will then be used to

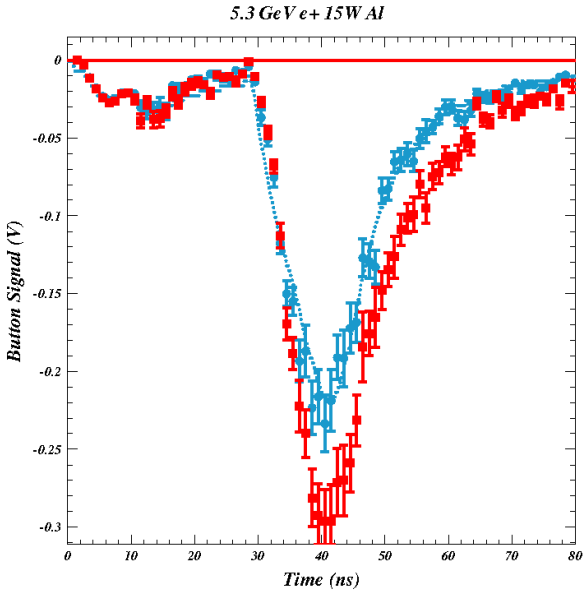

FIG. 11: *Effect of varying modeled horizontal beam position*: The signal produced when the beam is at -1.8 mm is shown in blue. The red plot shows the signal when the beam is at 2.2 mm (the "original" position of the beam).

help interpret the differences between the two data sets and measure the effects of conditioning on bare Al.

VII. ACKNOWLEDGEMENTS

I would like to acknowledge and thank the Cornell University Laboratory for Elementary-Particle Physics for hosting this program and the National Science Foundation for their support.

Special thanks to my mentor, J.A. Crittenden, for his help and guidance throughout this project. I also thank the organizers of this REU program including I. Bazarov, M. Wesley, and L. Hine.

---

[1] F. Zimmermann and G. Rumolo, *Electron Cloud Build Up in Machines with Short Bunches*. IFCA Beam Dynamics Newsletter No. 33, (April 2004).

[2] M.A. Furman and M.T.F. Pivi, *Probabilistic Model for the Simulation of Secondary Electron Emission*. Phys Rev ST-AB 5, 124404, (2002).

[3] J.A. Crittenden, Y. Li, M.A. Palmer, S. Santos, J.P. Sikora, S. Calatroni, G. Rumolo, S. Kato, *Time-Resolved Shielded-Pickup Measurements and Modeling of Beam Conditioning Effects on Electron Cloud Buildup at CesrTA*, proceedings of IPAC12, (May 2012).

[4] J.A. Crittenden, *Electron Cloud Buildup Characterization Using Shielded Pickup Measurements and Custom Modeling Code*. Proceedings of ECLOUD 2012: 5^{th} International Workshop on Electron-Cloud Effects, La Biodola, Elba, Italy, (June 2012).

[5] Private conversation with J. Crittenden, (26 June 2012)
[6] G. Rumolo and F. Zimmerman, *Practical User Guide for ECLOUD*. CERN-SL-Note-2002-016 (AP), (2002).
[7] Private conversation with J. Crittenden, (7 August 2012).